AGU PUBLICATIONS

JGR

Journal of Geophysical Research: Space Physics

RESEARCH ARTICLE
10.1002/2013JA019670

Key Points:
- VLF technique sensitivity detection limit
- Lower limit X-ray fluence is found in order to be detected by the VLF technique
- The illumination parameter is crucial for a given VLF propagation path

Correspondence to:
J.-P. Raulin,
raulin@craam.mackenzie.br

Citation:
Raulin, J.-P., G. Trottet, C. G. Giménez de Castro, E. Correia, and E. L. Macotela (2014), Nighttime sensitivity of ionospheric VLF measurements to X-ray bursts from a remote cosmic source, *J. Geophys. Res. Space Physics*, *119*, 4758–4766, doi:10.1002/2013JA019670.

Received 28 NOV 2013
Accepted 27 APR 2014
Accepted article online 2 MAY 2014
Published online 2 JUN 2014

Nighttime sensitivity of ionospheric VLF measurements to X-ray bursts from a remote cosmic source

Jean-Pierre Raulin[1], Gérard Trottet[2], C. Guillermo Giménez de Castro[1], Emilia Correia[1,3], and E. Liliana Macotela[1]

[1]Centro de Radio Astronomia e Astrofísica Mackenzie, CRAAM, Universidade Presbiteriana Mackenzie, São Paulo, Brazil, [2]Observatoire de Paris, Meudon, France, [3]Instituto Nacional de Pesquisas Espaciais, INPE, São José dos Campos, Brazil

Abstract On 22 January 2009, a series of X-ray bursts were emitted by the soft gamma ray repeater SGR J1550-5418. Some of these bursts produced enhanced ionization in the nighttime lower ionosphere. These ionospheric disturbances were studied using X-ray measurements from the Anti-Coincidence Shield of the Spectrometer for Integral onboard the International Gamma-Ray Astrophysics Laboratory and simultaneous phase and amplitude records from two VLF propagation paths between the transmitter Naval Radio Station, Pearl Harbor (Hawaii) and the receivers Radio Observatorio do Itapetinga (Brazil) and Estação Antarctica Commandante Ferraz (Antarctic Peninsula). The VLF measurements have been obtained with an unprecedented high time resolution of 20 ms. We find that the illumination factor I (illuminated path length times the cosine of the zenith angle), which characterizes the propagation paths underlying the flaring object, is a key parameter which determines the sensitivity threshold of the VLF detection of X-ray bursts from nonsolar transients. For the present VLF measurements of bursts from SGR J1550-5418, it is found that for $I \geq 1.8$ Mm, all X-ray bursts with fluence in the 25 keV to 2 MeV range larger than $F_{25\_min} \sim 1.0 \times 10^{-6}$ erg/cm^2 produce a measurable ionospheric disturbance. Such a lower limit of the X-ray fluence value indicates that moderate X-ray bursts, as opposed to giant X-ray bursts, do produce ionospheric disturbances larger than the sensitivity limit of the VLF technique. Therefore, the frequency of detection of such events could be improved, for example by increasing the coverage of existing VLF receiving networks. The VLF detection of high-energy astrophysical bursts then appears as an important observational diagnostic to complement their detection in space. This would be especially important when space observations suffer from adverse conditions, like saturation, occultation from the Earth, or the passage of the spacecraft through the South Atlantic anomaly.

1. Introduction

Very low frequency (VLF) waves can propagate over long distances within the Earth-ionosphere waveguide without suffering significant attenuation. Therefore, they can be used to monitor the electrical conductivity Ω of the lower ionosphere, which is characterized by the two Wait's parameters, namely, its reference height H (in km) and its sharpness β (in km^{-1}) [*Wait*, 1959; *Wait and Spies*, 1964]. Any disturbance of the low ionosphere that produces changes of these parameters will show up as phase and amplitude variations of the received VLF signal, $\Delta\Phi$ and ΔA, respectively. $\Delta\Phi$ and ΔA are changes with respect to the unperturbed phases and amplitudes.

Soft X-rays from solar flares are the more common sources of ionospheric disturbances which can be monitored using the VLF technique [*Bracewell and Straker*, 1949; *Thomson et al*., 2005; *Pacini and Raulin*, 2006; *Raulin et al*., 2006, 2010]. In addition to solar flares, there is a variety of solar-terrestrial events that can significantly change Ω and that can thus be studied by measuring the resulting $\Delta\Phi$ and ΔA. Electron precipitation caused by increased geomagnetic activity [*Abdu et al*., 1981] or induced by lightning [*Inan et al*., 1996] as well as transient meteor showers [*Chilton*, 1961; *Kaufmann et al*., 1989] constitute illustrative examples of such transient events.

Besides these solar-terrestrial events, the lower ionosphere can also be disturbed by nonsolar transients like gamma ray bursts (GRB) and soft gamma ray repeaters (SGR). Such outbursts from remote astrophysical objects produce large fluxes of energetic X-ray photons which can enter the neutral Earth atmosphere and produce significant changes of the electrical conductivity height profile between 20 and 80 km above the Earth's surface. So far, the detection of ionization excesses by using VLF observations has been reported for

only four events of this kind. The single γ ray burst GRB830801 was detected using several VLF propagation paths [*Fishman and Inan*, 1988], and the measured γ ray fluence was of 2×10^{-3} erg/cm^2 in the 5 keV to 7.5 MeV energy range. Another unique and single burst from SGR 1900+14 [*Hurley et al*., 1999; *Tanaka et al*., 2007] was also detected by using VLF networks in the US [*Inan et al*., 1999] and in Japan [*Tanaka et al*., 2008]. In this particular case, the VLF observations allowed constraining the low-energy photon spectrum in the absence of available X-ray data below 20 keV [*Inan et al*., 1999; *Tanaka et al*., 2008]. The third event reported was, again, an isolated outburst from SGR 1806-20. It was the largest burst ever observed, and it saturated most of the γ ray sensors in space [*Hurley et al*., 2005; *Palmer et al*., 2005]. The fluence above 50 keV integrated over the short (600 ms) initial and main peak was as large as 2 erg/cm^2 [*Terasawa et al*., 2005; *Inan et al*., 2007]. This giant flare from SGR 1806-20 was also detected using an extremely low frequency diagnostic [*Tanaka et al*., 2011]. The last event occurred on 22 January 2009 when SGR J1550-5418 released hundreds of bursts between 00:00 and 09:00 UT [*Mereghetti et al*., 2009], in contrast to the single-burst examples mentioned above. The South America VLF Network [*Raulin et al*., 2009] clearly detected the ionospheric disturbances produced by eight of these X-ray bursts [*Tanaka et al*., 2010].

It has been unclear if the small number of VLF detections of ionospheric disturbances produced by cosmic γ ray bursts reported so far is principally due to the low sensitivity of the VLF technique, to the lack of a systematic search for such disturbances, to a (too) small coverage of the Earth surface by VLF instrumental networks, or to a too low time resolution of the VLF measurements (generally 1 s). The main goal of the present study is to address the nighttime sensitivity of the VLF response to a series of X-ray bursts emitted by SGR J1550-5418 and detected by the Anti-Coincidence Shield (ACS) of the Spectrometer for Integral (SPI) onboard International Gamma-Ray Astrophysics Laboratory (INTEGRAL) between 04:15 and 08:20 UT on 22 January 2009. Section 2 describes the instrumentation used and the data analysis performed on VLF measurements obtained with two propagation paths from Hawaii to Brazil and to the Antarctica peninsula, with different illumination conditions and a time resolution of 20 ms. The results are presented in section 3. The final section presents a discussion of the observational findings and some concluding remarks.

2. Instrumentation and Data Analysis

We have used X-ray observations obtained with ACS/SPI (http://www.isdc.unige.ch/integral/science/grb#ACS) which provided uninterrupted monitoring of SGR J1550-5418 on 22 January 2009, during the VLF observation window considered here (04:15 UT–08:20 UT). During this period of time, 55 X-ray bursts from SGR J1550-5418 were detected by ACS/SPI which measures the integral X-ray counts above some threshold energy (~80 keV) with a time bin of 50 ms. For each burst the total number of counts C was obtained by integrating the background-subtracted integral count rate over the burst duration, defined as the time interval during which the integral count rate is $3\sigma_X$ above the background. In order to compare ACS/SPI and VLF light curves, the UT time ACS/SPI measurements at the Earth's surface has been derived from the UT time at the INTEGRAL satellite according to the position of the satellite at the time of the burst occurrence and the right ascension and declination of SGR J1550-5418. In addition, we have taken into account the distance between the subflare point and the VLF propagation paths, as well as the propagation time of the perturbation onset between NPM and the VLF receivers.

The VLF data used in this study were obtained using two propagation paths between the transmitter NPM (Lualualei, Hawaii, 21.4 N, 158.15 W, frequency = 21.4 kHz) and the receivers ROI (Radio Observatorio do Itapetinga, 23.18 S, 46.55 W) and EACF (Estação Antarctica Commandante Ferraz, 62.72 S, 29.72 W). The two VLF receivers are part of the Atmospheric Weather Electromagnetic System for Observation Modeling and Education array [*Cohen et al*., 2009]. The total length of the propagation path is $L_{ROI} = 13{,}071$ km for NPM-ROI and $L_{EACF} = 12{,}660$ km for NPM-EACF. The VLF observation time window adopted here is 04:15 UT–08:20 UT. The starting time 04:15 UT corresponds to the time when the sunset terminator line crosses the location of the transmitter NPM, insuring that the propagation undergoes nighttime conditions. After 08:20 UT no bursts were detected by ACS/SPI on 22 January 2009. Figure 1 shows the propagation paths on 22 January 2009 at 05:18 UT (white lines), the projection on the surface of the Earth of the Sun's position (yellow circle), and the subflare point (black circle). Solar nighttime and daytime conditions are illustrated using dark blue and light blue areas, respectively. The SGR J1550-5418 terminator line defined by the direction of the flaring object is shown by the black line. The VLF amplitude and phase were measured at ROI and EACF with a time

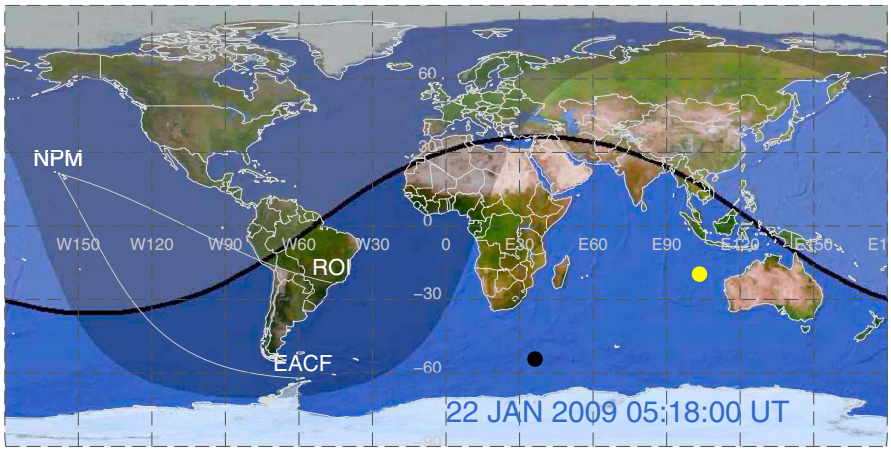

Figure 1. The white lines show the NPM-EACF and NPM-ROI VLF propagation paths on 22 January 2009 at 05:18 UT. The black and yellow circles represent, respectively, the projections of the subflare point and of the Sun on the Earth's surface. The dark and light blue areas indicate, respectively, the regions under nighttime conditions and under solar illumination. The regions of the Earth illuminated by the flaring object are located south of the thick black line.

resolution of 20 ms. In the following we will only consider the amplitude. During an X-ray burst, the maximum change, ΔA, of the received amplitude is considered as significant when it exceeds a value of $3\sigma_{VLF}$, where σ_{VLF} is the RMS of the mean undisturbed level A_0 before the amplitude change. A_0 depends on the path length, the nighttime ionospheric reference height, i.e., the propagation path position relative to the Sun terminator line, and whether the wave propagates over the sea or land [*Watt*, 1967]. In the following we thus consider the relative variations $\Delta A/A_0$ which are independent of these effects. In addition, the amount of amplitude changes is also dependent on the length L of the path illuminated by the X-ray disturbance and on the direction of the incoming radiation. Therefore, in order to compare the ionospheric response observed with the two VLF propagation paths, the values $\Delta A/A_0$ have been divided by the illumination factor $I = L\cos(\chi)$ to obtain $\Delta A/A_0/I$ where χ is the mean zenith angle estimated along the portion L. The path NPM-ROI was totally under nighttime conditions for the whole period considered, and the illumination factor varied in the range $I_{ROI} = (0.2–2.6)$ Mm. At about 07:15 UT the daytime terminator line crossed the EACF receiver location, and the path NPM-EACF began to be partly illuminated by solar radiation. The illumination factor I varied in the range $I_{EACF} = (1.8–2.95)$.

Between 04:15 UT and 08:20 UT 55 X-ray bursts were observed from ACS/SPI data, which produced 17 and 39 significant amplitude variations in the NPM-ROI and NPM-EACF records, respectively. These have been classified as "simple (S)" or "complex (C)." Ten and 16 amplitude variations were identified as simple from NPM-ROI and NPM-EACF data, respectively. An example of a simple burst is illustrated in Figure 2. It is characterized by a single peak in X-ray associated with a fast decrease of the relative VLF amplitude, followed by a slower increase till it recovers the undisturbed level. Similarly, 7 and 23 complex events were observed using NPM-ROI and NPM-EACF data, respectively. Figure 3 shows that a complex event consists in an X-ray burst with several peaks associated with multiple decreases of the VLF relative amplitude. Figure 3 shows that, except for the first burst at 05:17:43.6 UT, the subsequent relative amplitude decreases occurred most often during the recovery phase of a preceding burst.

Table 1 displays the characteristics of the 55 X-ray bursts detected by ACS/SPI and the measured $\Delta A/A_0$ using the data from the two VLF propagation paths. Although not discussed in this paper we have also determined the maximum phase changes $\Delta\Phi$ with respect to the unperturbed phase before the corresponding X-ray burst. For each X-ray burst, the first three columns indicate its starting time, its duration, and its fluence F_{25} in the 25 keV to 2 MeV energy range. The remaining six columns display, for each VLF propagation path, the relative changes of the amplitudes $\Delta A/A_0$, the phase changes $\Delta\Phi$ as well as the corresponding $3\sigma_{VLF}$ level in parenthesis, and whether the bursts are simple (S), complex (C), or not detected (-). F_{25} has been estimated by using former results obtained by *Mereghetti et al.* [2009]. These authors have computed the full ACS/SPI instrumental response (effective area as a function of energy) for observations of SGR J1550-5418 between 02:46 and 08:18 UT on 22 January 2009. Furthermore, since ACS/SPI has no energy resolution, they assumed

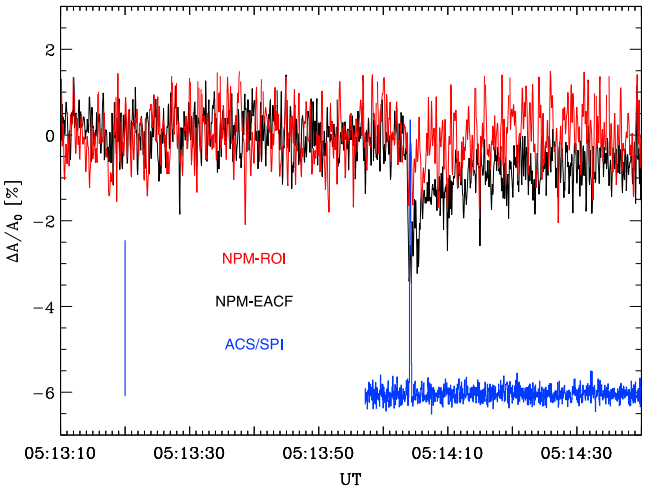

Figure 2. Example of a simple VLF amplitude decrease observed at EACF (black curve). At ROI (red curve), the amplitude change is below the significance criterion. The blue curve shows the time evolution of the associated X-ray count rate measured by ACS/SPI. The blue vertical line on the left represents an ACS/SPI count rate of 4×10^4 counts/s

that the X-ray spectrum of each burst is well represented by an optically thin thermal bremsstrahlung spectrum (OTTB) with $kT = 40$ keV, where k is the Boltzmann constant and T the temperature. A test count spectrum is then obtained by convolving the OTTB photon spectrum with the ACS/SPI response. A test ACS/SPI-INTEGRAL rate is computed by integrating the test count spectrum over energy. For each burst, the ratio between the observed and test integral rates provides the absolute normalization of the adopted OTTB photon spectrum which can then be used to derive the burst X-ray fluence in any given energy range. Using this procedure, *Mereghetti et al.* [2009] have estimated the X-ray fluence F_{25} for nine of the simple bursts listed in Table 1. Using these values, we have determined a conversion factor K from total counts C to F_{25} (erg cm^{-2}) by setting $K = F_{25}^{mean}/C^{mean}$, where F_{25}^{mean} and C^{mean} are, respectively, the means of the F_{25} and C for the nine simple bursts in common with *Mereghetti et al.* [2009].

3. Observational Results

The fluence F_{25} of each of the 55 X-ray bursts listed in Table 1 is displayed as a function of time in Figure 4a using a green or a red diamond depending on whether or not the burst is detected in the VLF signal measured using the NPM-EACF propagation path. The black curve shows the illumination I_{EACF}. Figure 4b is the same as Figure 4a for the NPM-ROI propagation path. Examination of Figures 4a and 4b results in the following comments:

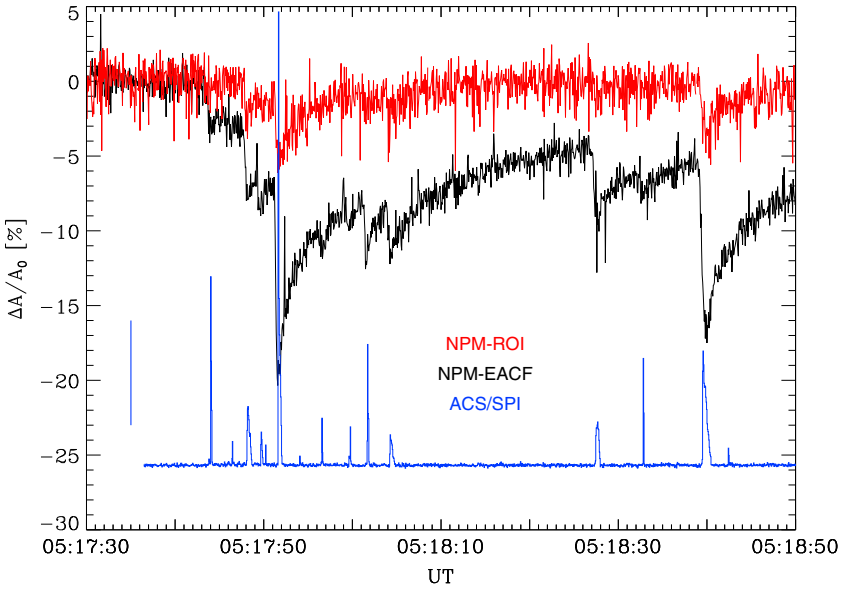

Figure 3. Same as Figure 2 for complex bursts. The vertical blue line on the left represents an ACS/SPI count rate of 2×10^5 counts/s.

Table 1. Burst Properties Observed on 22 January 2009 From SGR J1550-5418

Time (UT)	Duration (s)	Fluence $\times 10^{-5}$ (erg/cm^{-2})	$\Delta A/A_0$ EACF (%)	$\Delta\Phi$ EACF (deg)	Class	$\Delta A/A_0$ ROI (%)	$\Delta\Phi$ ROI (deg)	Class
04:34:53.3	0.551	0.1528	1.50 (1.50)	-	S	-	-	-
04:39:04.9	1.100	1.1098	7.8 (1.6)	2.1 (0.9)	C	-	-	-
04:42:03.0	0.151	0.0558	-	-	-	-	-	-
04:43:05.7	0.050	0.0215	-	-	-	-	-	-
04:53:15.4	0.149	0.1133	1.7 (1.2)	-	C	-	-	-
04:53:24.8	0.150	0.1017	-	-	-	-	-	-
04:53:43.9	0.151	0.0234	-	-	-	-	-	-
04:54:22.9	0.050	0.0231	-	-	-	-	-	-
04:57:19.5	0.299	0.1033	1.3 (1.2)	-	S	-	-	-
04:57:29.4	0.800	0.3972	4.5 (1.4)	-	S	-	-	-
04:58:02.6	0.199	0.2323	1.9 (1.2)	-	S	-	-	-
05:14:03.8	0.350	0.2227	3.2 (1.4)	-	S	-	-	-
05:17:43.6	0.201	0.4833	3.0 (1.7)	-	S	-	-	-
05:17:46.1	0.100	0.0422	-	-	-	-	-	-
05:17:47.8	0.600	0.5213	5.7 (1.7)	1.5 (1.2)	C	2.2 (1.4)	-	S
05:17:49.3	0.249	0.1406	2.9 (1.2)	-	C	-	-	-
05:17:51.3	0.450	1.9012	14.6 (1.2)	1.8 (0.9)	C	3.9 (1.0)	2.5 (1.2)	C
05:17:56.2	0.152	0.0871	1.4 (1.1)	-	C	-	-	-
05:17:59.4	0.251	0.0918	1.8 (1.2)	-	C	-	-	-
05:18:01.3	0.251	0.3406	5.1 (1.5)	1.3 (0.9)	C	-	-	-
05:18:03.9	0.550	0.2449	4.0 (1.5)	-	C	-	-	-
05:18:27.3	0.550	0.0426	5.8 (1.2)	-	C	-	-	-
05:18:32.4	0.100	0.2192	1.9 (1.1)	-	C	-	-	-
05:18:39.2	1.001	1.4279	12.9 (1.3)	1.6 (0.9)	C	4.0 (1.5)	1.9 (1.5)	S
05:18:42.0	0.100	0.0371	-	-	-	-	-	-
05:26:52.5	0.251	0.3559	3.3 (1.2)	-	S	-	-	-
06:38:27.6	0.350	0.2677	4.5 (2.1)	-	S	2.8 (1.5)	-	S
06:38:56.1	0.199	0.0310	-	-	-	-	-	-
06:41:01.9	1.001	2.3364	16.8 (1.7)	1.4 (1.2)	S	9.1 (1.5)	2.3 (1.2)	S
06:43:05.4	0.150	0.0482	-	-	-	-	-	-
06:43:47.8	0.351	0.2006	4.2 (1.6)	-	S	2.3 (1.6)	-	S
06:44:15.6	0.102	0.0595	-	-	-	-	-	-
06:44:36.1	1.799	1.9116	15.5 (1.8)	2.1 (0.9)	S	9.5 (1.3)	2.9 (0.9)	S
06:44:59.9	0.201	0.2097	2.5 (1.4)	-	C	-	-	-
06:45:12.0	0.201	0.1810	3.2 (1.6)	-	C	1.8 (1.5)	-	C
06:45:13.6	1.450	4.5486	30.7 (1.6)	4.4 (0.9)	C	18.2 (1.5)	6.3 (1.5)	C
06:47:56.7	0.350	1.8061	15.2 (2.0)	1.8 (1.2)	S	10.7 (1.6)	2.2 (1.2)	S
06:47:57.2	0.150	0.0710	-	-	-	-	-	-
06:48:00.0	0.249	0.2017	2.9 (1.1)	-	C	-	-	-
06:48:01.4	1.500	0.0532	-	-	-	-	-	-
06:48:02.5	0.150	0.1674	3.2 (2.1)	-	C	-	-	-
06:48:04.1	8.149	27.543	57.9 (1.6)	17.3 (1.8)	C	36.9 (2.3)	28.3 (1.5)	C
06:48:14.9	0.850	0.5747	5.3 (1.6)	-	C	2.6 (2.3)	-	C
06:48:21.2	0.100	0.0465	-	-	-	-	-	-
06:48:21.5	0.151	0.1126	4.9 (1.4)	-	C	-	-	-
06:48:37.4	0.500	0.2891	5.8 (1.2)	-	C	3.1 (1.8)	-	C
06:49:48.6	0.350	0.8323	5.4 (1.7)	-	C	2.7 (1.55)	-	C
06:50:57.3	0.200	0.0920	-	-	-	-	-	-
06:59:35.6	0.251	0.0684	-	-	-	-	-	-
07:00:58.8	0.150	0.0602	-	-	-	-	-	-
07:05:56.5	0.350	0.4588	4.5 (1.6)	-	S	4.2 (2.6)	-	S
07:31:15.0	0.349	0.3083	3.5 (2.6)	-	S	2.7 (1.7)	-	S
07:49:40.5	0.400	0.2225	6.5 (2.8)	-	S	4.6 (1.6)	-	S
08:13:50.8	0.400	0.1202	5.5 (3.3)	-	C	4.0 (2.3)	-	C
08:17:29.7	6.903	6.6081	33.8 (2.7)	3.8 (1.2)	S	25.0 (2.1)	9.4 (1.2)	S

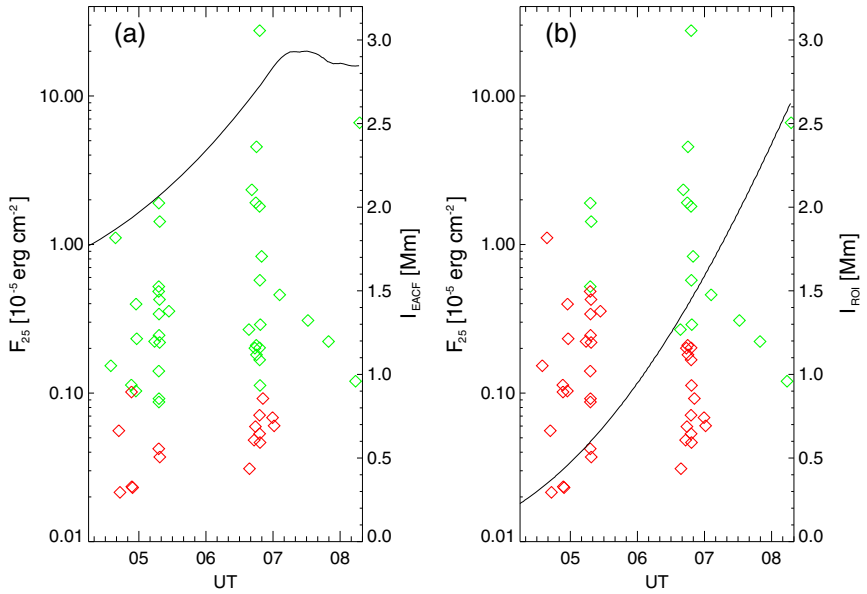

Figure 4. The X-ray fluence F_{25} as a function of time for the 55 bursts observed and producing (green diamonds) or not producing (red diamonds) a significant ionospheric disturbance using (a) NPM-EACF and (b) NPM-ROI propagation paths. For each path, the illumination factor is shown by the black curve.

1. For the NPM-EACF propagation path, the illumination factor I_{EACF} is always higher than 1.8 Mm; no VLF amplitude changes are detected for $F_{25} < F_{25\_min} \sim 10^{-6}$ erg/cm^2; this value of F_{25_min} is independent of I_{EACF}.
2. For the NPM-ROI propagation path, the illumination factor I_{ROI} increases with time from 0.2 to 2.6 Mm; the minimum value of F_{25} decreases with increasing I_{ROI}, reaching $F_{25\_min} \sim 10^{-6}$ erg/cm^2 for an illumination of about 1.8 Mm, consistently with the NPM-EACF data.

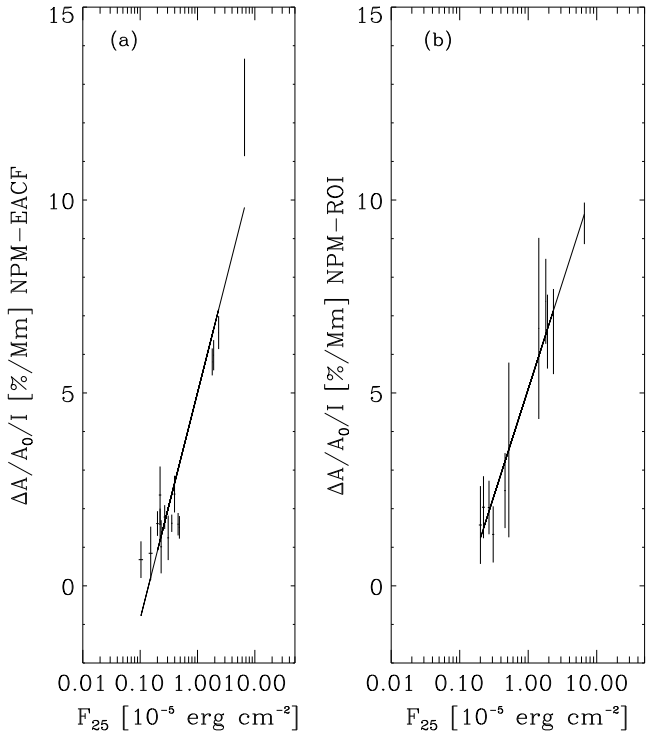

Figure 5. $\Delta A/A_0/I$ versus F_{25} for the simple bursts detected using (a) NPM-EACF and (b) NPM-ROI propagation paths data. The straight lines show the linear regression lines which fit the data. The error bars correspond to $3K\sigma_X$ and $3\sigma_{VLF}/I$ uncertainties for the X-ray and VLF data, respectively (see text).

Table 1 and Figures 2 to 4 indicate that more VLF amplitude decreases were identified in the NPM-EACF propagation path compared to the NPM-ROI path in response to the X-ray bursts detected by ACS/SPI. This can be understood as mainly due to the time variation of the illumination factors, as shown in Figures 4a and 4b. For example, between 05:13 and 05:19 UT, when I_{EACF} is about 3 times larger than I_{ROI}, the "simple burst" detected using NPM-EACF is not detected by using NPM-ROI (see Figure 2). Similarly, while 13 bursts were detected using NPM-EACF, only three were recorded using NPM-ROI (see Figure 3). When both I_{ROI} and I_{EACF} are larger than or equal to ~1.8 Mm, i.e., after ~07:06 UT, the same number of bursts is detected for both paths (cf. Table 1 and Figure 4).

$\Delta A/A_0/I$ is plotted as a function of F_{25} in Figure 5 for all the simple bursts detected on the two VLF propagation paths. $\Delta A/A_0/I$ and F_{25} are strongly correlated, the coefficient of correlation being 0.97 ± 0.02 and 0.91 ± 0.07 for the NPM-ROI and NPM-EACF propagation paths, respectively. Figure 5 also shows that for both paths the linear regression lines point to $F_{25\_min} \sim 10^{-6}$ erg/cm^2 for $\Delta A/A_0/I \sim 0$. This indicates that X-ray bursts with $F_{25} < F_{25\_min}$ do not produce significant amplitude variations independently of the propagation path. This value of F_{25_min} is consistent with that inferred above by using Figure 4.

Finally, we note that the difference between the starting time of a given VLF amplitude decrease and the onset time of the associated X-ray burst is about 50 ms, that is, the time bin of ACS/SPI data.

4. Discussion and Concluding Remarks

In this study we have analyzed the ionospheric response to X-ray bursts from SGR J1550-5418 during nighttime conditions on 22 January 2009 between 04:15 and 08:20 UT. We have used VLF measurements obtained for two propagation paths, NPM-ROI and NPM-EACF, for which the illumination varies with time during the considered period. The response of the lower ionosphere to an X-ray burst has been characterized by the relative amplitude change $\Delta A/A_0$ of the received VLF signal. Our results indicate that the occurrence of VLF detection of the less intense X-ray burst increases with the illumination I until it reaches a value of about 1.8 Mm. Indeed, before ~ 07:06 UT much fewer X-ray bursts are detected by using the NPM-ROI path ($I_{ROI} < 1.8$ Mm) than by using the NPM-EACF path ($I_{EACF} > 1.8$ Mm). On the other hand, after 07:06 UT when both I_{ROI} and I_{EACF} are larger than 1.8 Mm, the same number of X-ray bursts is detected using the two propagation paths (see Figure 4 and Table 1). Therefore, for $I < 1.8$ Mm, only the larger X-ray bursts can be detected by VLF measurements. However, for $I > 1.8$ Mm, the VLF detection becomes independent of the illumination, and the minimum X-ray fluence F_{25_min} needed to produce a significant ionospheric disturbance is found to be $\sim 10^{-6}$ erg/cm^2. For simple bursts, F_{25} and $\Delta A/A_0/I$ are strongly correlated (coefficient of correlation > 0.92) so that Log(F_{25}) is approximately proportional to $\Delta A/A_0/I$. Consistently, such a relationship also leads to $F_{25\_min} \sim 10^{-6}$ erg/cm^2. Therefore, for a given propagation path it appears that the sensitivity of the VLF technique in detecting X-ray bursts increases with the illumination factor I, that is, with increasing the illuminated distance L and decreasing zenith angle χ. A general result of the present work is that, for a given external source, the best sensitivity of the VLF detection of the ionospheric response to X-rays bursts is reached for illumination factors larger than a minimum one, I_{min}, which is independent of the VLF propagation path. I_{min} is then related to the lowest ionospheric ionization excess caused by the fluence F_{25_min} capable of producing a significant VLF response.

The number of VLF amplitude changes detected using the path NPM-ROI is larger than that reported in *Tanaka et al.* [2010] using 1 s time resolution. This is due to the fact that all the small VLF amplitude changes ($\Delta A < 5$ dB), measured in the present study with a time resolution of 20 ms, reach their maximum variation in less than 1 s. Therefore, with a time resolution of 1 s they are blurred and do not appear as significant anymore. As a consequence, in *Tanaka et al.* [2010], only the eight larger VLF amplitude decreases were detected.

Two hundred eighty-six bursts from SGR J1550-5418 were also detected with the *FERMI* Gamma Ray Burst Monitor (GBM) [*van der Horst et al.*, 2012]. A detailed spectral analysis was performed in the 8–200 keV energy range. Different shapes of the incident photon spectrum are found consistent with data, including the OTTB spectrum with $kT = 39$ keV, similar to that assumed by *Mereghetti et al.* [2009] and used in this work to compute F_{25}. However, all the VLF amplitude decreases presented here and occurring during *FERMI* observing times corresponded to X-ray bursts which saturated the NaI GBM detectors. The distribution of unsaturated burst fluences detected by *FERMI* in the 8 keV to 1 MeV range [see *van der Horst et al.*, 2012, Figures 6 and 7] indicates a clear rollover at about 2×10^{-6} erg/cm^2, above which most of the X-ray bursts saturated the GBM detectors. Using the OTTB photon spectrum, this fluence corresponds to $F_{25} \sim 1.3 \times 10^{-6}$ erg/cm^2, which, by chance, is close to the VLF detection limit $F_{25\_min} \sim 10^{-6}$ erg/cm^2 determined in the present work. Then it appears *FERMI* and VLF measurements provide complementary tools to detect X-ray bursts from nonsolar transients like SGR J1550-5418 since the minimum X-ray fluence needed to produce a ionospheric response corresponds approximately to the fluence above which the NaI GBM detectors are saturated.

Pacini and Raulin [2006] have shown that maximum VLF phase changes produced by solar flares are strongly correlated to the X-ray fluence above 6 keV integrated between the start time of the X-rays and the peak time of the phase changes. In order to estimate the minimum soft >6 keV X-ray fluence F_{s_min} of solar flares needed to disturb the *D* region of the ionosphere, we have used the method described in *Pacini and Raulin* [2006] to determine the X-ray flux F_X above 6 keV. Seventeen solar flares of classes ranging from C1.7 to M3.0 producing VLF phase advances have been analyzed. For each flare, the starting times t_X and t_{VLF} of the X-ray burst and of the corresponding phase change, defined as the initial instants when both quantities differ by 3σ from the unperturbed level, have been measured. The minimum fluence F_{s_min} was then obtained by integrating F_X between t_X and t_{VLF}. The results obtained for the 17 solar flares show that F_{s_min} lies in the range $0.7–2.6\times10^{-4}$ erg/cm^2. For nonsolar X-ray bursts, using the OTTB photon spectrum mentioned earlier, we find that $F_{25\_min}\sim10^{-6}$ erg/cm^2 corresponds to a minimum fluence $F_{6\_min}\sim1.8\times10^{-6}$ erg/cm^2 above 6 keV. This is at least 2 orders of magnitude lower than F_{s_min}. This emphasizes, as expected, that the ionospheric plasma is much less sensitive during daytime when illuminated by the solar radiation compared to nighttime conditions. It should be noted that the value found for F_{s_min} indicates that only the stronger bursts can be detected during daytime ionospheric conditions, when the VLF propagation paths are partially or totally under the influence of the solar radiation [*Inan et al.*, 1999, 2007]. In the present case, the X-ray burst at 06:48:04 UT would have produced an ionospheric disturbance large enough to be detected by the VLF technique during daytime.

The time delays reported between the onset times of the X-ray bursts and the amplitude decreases are of the order of the ACS/SPI time resolution. Therefore, one can say that the response of the ionosphere is almost simultaneous to the X-ray disturbances. In contrast the response of the daytime ionosphere to incoming photons from a solar flare can vary from one to a few minutes [e.g., see *Raulin et al.*, 2010, Figure 2]. This reflects the fact that the nighttime ionospheric plasma is much more sensitive to external disturbances compared to daytime conditions. At night, the electrical conductivity at ~70 km altitude, which is proportional to the ratio of the plasma frequency squared and the electron (neutral) collision frequency, is reduced by ~2 orders of magnitude from 10^5 to 10^3 s^{-1} [*Wait and Spies*, 1964]. Then, a given relative change of the electron density $\Delta N/N_{amb}$ produced by photo-ionization requires a higher excess ΔN during daytime than during nighttime to produce a change in VLF wave amplitude. A further reason is that the X-ray flux rises more slowly during a solar flare than during a cosmic burst. Therefore, the minimum X-ray fluence needed to produce a VLF response is reached faster.

In summary, we have taken advantage of the occurrence of the bursting period of SGR J1550-5418 on 22 January 2009 between 00:00 and 09:00 UT when ACS/SPI-INTEGRAL detected hundreds of X-ray bursts. This is a unique event in the sense that previous such SGR ionospheric disturbances detected using the VLF technique were rare. Only four cases, three of them being due to giant X-ray flares, have been reported in the literature. We have shown the key importance of the illumination of the VLF propagation paths for the sensitivity of the detection of the subsequent ionospheric disturbances. For the two propagation paths used in this work we have found that an incident minimum X-ray fluence of $F_{25\_min}\sim10^{-6}$ erg/cm^2 is necessary to disturb the nighttime ionosphere. As expected, this is well below the minimum fluence needed to affect the daytime ionosphere. The fact that the nighttime ionosphere can be disturbed by intermediate cosmic X-ray bursts, and not only by giant ones, indicates that the frequency of detection of such events could be improved, for example, by increasing the coverage of existing VLF receiving networks, decreasing the receiver noise levels, and performing a systematic search. The VLF detection of high-energy astrophysical bursts appears as an interesting observational diagnostic that complements their detection in space, in particular when space observations are not available, for example, during Earth's occultation or above the South Atlantic Anomaly region, or suffer from saturation.

Acknowledgments

J.P.R. would like to thank funding agencies CNPq (proc. 305655/2010-8) and FAPESP (procs. 2006/02979-0 and 2011/24117-9). G.T. thanks CNPq and CNRS funding agencies (proc. 490444/2010-5). E.C. thanks CNPq/PROANTAR (proc. 0520186/06-0, 556872/2009-6, 374956/2010-3, 374958/2010-6, and 374957/2010-0) and INCT-APA (Instituto Nacional de Ciência e Tecnologia Antártico de Pesquisas Ambientais, CNPq proc.574018/2008-5 and FAPERJ proc. E-16/170.023/2008). The authors thank two anonymous referees for valuable comments.

Philippa Browning thanks the reviewers for their assistance in evaluating this paper.

References

Abdu, M. A., S. Ananthakrishnan, E. F. Coutinho, B. A. Krishnan, and E. M. Reis (1981), Azimuthal drift and precipitation of electrons into the South Atlantic geomagnetic anomaly during SC magnetic storm, *J. Geophys. Res.*, *78*, 5830–5838, doi:10.1029/JA078i025p05830.

Bracewell, R. N., and T. W. Straker (1949), The study of solar flares by means of very long radio waves, *Mon. Not. R. Astron. Soc.*, *109*, 28–45.

Chilton, C. J. (1961), VLF phase perturbation associated with meteor shower ionization, *J. Geophys. Res.*, *66*, 379–383, doi:10.1029/JZ066i002p00379.

Cohen, M. B., U. S. Inan, and E. P. Paschal (2009), Sensitive broadband ELF/VLF radio reception with the AWESOME instrument, *IEEE Trans. Geosci. Remote Sens.*, doi:10.1109/TGRS.2009.2028334.

Fishman, G. J., and U. S. Inan (1988), Observation of an ionospheric disturbance caused by a gamma-ray burst, *Nature*, *331*, 418–420.

Hurley, K., et al. (1999), A giant periodic flare from the soft γ-ray repeater SGR1900+14, *Nature*, *397*(6714), 41–43.

Hurley, K., et al. (2005), An exceptionally bright flare from SGR 1806-20 and the origins of short-duration γ-ray bursts, *Nature*, *434*(7037), 1098–1103.

Inan, U. S., A. Slingeland, V. P. Pasko, and J. V. Rodriguez (1996), VLF and LF signatures of mesospheric/lower ionospheric response to lightning discharges, *J. Geophys. Res.*, *101*, 5219–5238, doi:10.1029/95JA03514.

Inan, U. S., N. G. Lehtinen, S. J. Lev-Tov, M. P. Johnson, T. F. Bell, and K. Hurley (1999), Ionization of the lower ionosphere by γ-rays from a magnetar: Detection of a low energy (3–10 keV) component, *Geophys. Res. Lett.*, *26*, 3357–3360, doi:10.1029/1999GL010690.

Inan, U. S., N. G. Lehtinen, R. C. Moore, K. Hurley, S. Boggs, D. M. Smith, and G. J. Fishman (2007), Massive disturbance of the daytime lower ionosphere by the giant γ-ray flare from magnetar SGR 1806-20, *Geophys. Res. Lett.*, *34*, L08103, doi:10.1029/2006GL029145.

Kaufmann, P., V. L. R. Kuntz, N. M. Paes Leme, L. R. Piazza, and J. W. S. Vilas Boas (1989), Effects of the large June 1975 meteoroid storm on Earth's ionosphere, *Science*, *246*, 787–790.

Mereghetti, S., et al. (2009), Strong bursts from the anomalous X-ray pulsar IE 1547.0-5408 observed with the *INTEGRAL/SPI* anti-coincidence shield, *Astrophys. J.*, *606*, L74–L78.

Pacini, A. A., and J.-P. Raulin (2006), Solar X-ray flares and ionospheric sudden phase anomalies relationship: A solar cycle phase dependence, *J. Geophys. Res.*, *111*, A09301, doi:10.1029/2006JA011613.

Palmer, D. M., et al. (2005), A giant γ-ray flare from the magnetar SGR 1806 - 20, *Nature*, *434*(7037), 1107–1109.

Raulin, J.-P., A. A. Pacini, P. Kaufmann, E. Correia, and M. A. G. Martinez (2006), On the detectability of solar X-ray flares using very low frequency sudden phase anomalies, *J. Atmos. Sol. Terr. Phys.*, *68*, 1029–1035.

Raulin, J.-P., P. David, R. Hadano, A. C. V. Saraiva, E. Correia, and P. Kaufmann (2009), The South America VLF NETwork (SAVNET), *Earth Moon Planets*, *104*, 247–261.

Raulin, J.-P., et al. (2010), Solar flare detection sensitivity using the South America VLF Network (SAVNET), *J. Geophys. Res.*, *115*, A07301, doi:10.1029/2009JA015154.

Tanaka, Y. T., T. Terasawa, N. Kawai, A. Yoshida, I. Yoshikawa, Y. Saito, T. Takashima, and T. Mukai (2007), Comparative study of the initial spikes of soft gamma-ray repeater giant flares in 1998 and 2004 observed with Geotail: Do magnetospheric instabilities trigger large-scale fracturing of a magnetar's crust?, *Astrophys J. Lett.*, *665*, L55–L58.

Tanaka, Y. T., J.-P. Raulin, F. C. P. Bertoni, P. R. Fagundes, J. Chau, N. J. Schuch, M. Hayakawa, Y. Hobara, T. Terasawa, and T. Takahashi (2010), First very low frequency detection of short repeated bursts from magnetar SGR J1550-5418, *Astrophys J. Lett.*, *721*, L24–L27.

Tanaka, Y. T., T. Terasawa, M. Yoshida, T. Horie and M. Hayakawa (2008), Ionospheric disturbances caused by SGR 1900+14 giant gamma ray flare in 1998: Constraints on the energy spectrum of the flare, *J. Geophys. Res.*, *113*, A07307, doi:10.1029/2008JA013119.

Tanaka, Y. T., et al. (2011), Detection of transient ELF emission caused by the extremely intense cosmic gamma-ray flare of 27 December 2004, *Geophys. Res. Lett.*, *38*, L08805, doi:10.1029/2011GL047008.

Terasawa, T., et al. (2005), Repeated injections of energy in the first 600ms of the giant flare of SGR1806 - 20, *Nature*, *434*(7037), 1110–1111.

Thomson, N. R., C. J. Rodger, and M. A. Clilverd (2005), Large solar flares and their ionospheric *D*-region enhancements, *J. Geophys. Res.*, *110*, A06306, doi:10.1029/2005JA011008.

van der Horst, A. J., et al. (2012), SGR J1550-5418 bursts detected with the Fermi Gamma-Ray Burst Monitor during its most prolific activity, *Astrophys. J.*, *749*, 122.

Wait, J. R. (1959), Diurnal change of ionospheric heights deduced from phase velocity measurements at VLF, *Proc. IRE*, *47*, 998.

Wait, J. R., and K. Spies (1964), Characteristics of the Earth-ionosphere waveguide for VLF radio waves, *NBS Technical Note U.S.*, 300.

Watt, A. D. (1967), *V.L.F. Radio Engineering, International Series of Monograph in Electromagnetic Waves*, chap. III, Pergamon Press, Oxford, U. K.